NUMERICAL STUDY ON THE EFFECT OF INERT REGION ON MASS TRANSFER BY THE SEGMENTED ELECTRODES IN LIMITING CURRENT METHOD

Woo Sik KIM, Joong Kon PARK and Ho Nam CHANG***

Korea Gas Corporation, Seoul, Korea
**Dept. of Chemical Engineering, Kyungpook National University, Taegu 630, Korea
*Dept. of Chemical Engineering, KAIST, P.O. Box 131, Cheongryang, Seoul, Korea
(Received 16 September 1986 • accepted 2 December 1986)

Abstract—The effect of inert region on mass transfer has been studied numerically for the cathode package that is used to measure the local mass transfer rate to a solid surface in a flow system. The inert region introduces a considerable error in the limiting current method as the region increased.

The overall mean Sherwood number on the cathodic electrodes with the inert region was correlated as follows.

$$Sh_m = 13.96\ Re^{0.339}\ (1+RT)^{0.444}$$

when RT is the ratio of the inert region to the active region. If RT is less than 0.25, the error of theoretical value to Leveque solution is less than 12%.

INTRODUCTION

The limiting current technique is one of the most widely used methods in measuring liquid-solid mass transfer rate [1-3]. However, the presence of inert region on the segmented electrodes is bound to include error in the measurement of local mass transfer rates. The cathode package is composed of several small electrodes that have to be electrically insulated alternately. The part of the insulation between the cathodes is the inert region where no electrochemical reaction occurs. In the measurement of the limiting current the growth of the concentration boundary layer stops where the inert region begins. Thus the current measured at the following electrode will be higher than without the presence of the inert region.

Chang et al. [4] studied numerically the mass transfer rate distribution on several active and inert regions arranged alternately between two-dimensional parallel plates. Sonin et al. [5] investigated the mass transfer in a long channel with the assumption of the second-order concentration profile within the diffusion layer. Two cases were considered: mass transfer in the developing region where the concentration diffusion layer is growing and in the developed region where the diffusion layer fills the channel. For the mass transfer in the U-turn of an electrodialyzer Kim et al. [6] studied the problem more accurately with the third-order concentration profile.

The effect of the inert region on the mass transfer rate over the short distance, however, has not been yet studied theoretically or experimentally in detail. Considering the fact that the electrodes used in actual measurement is relatively short compared to a characteristic dimension of the system, it would be useful to find a correlation that can describe the mass transfer on the segmented electrodes.

NUMERICAL ANALYSIS

As shown in Fig. 1, when the undirectional laminar flow between two-dimensional parallel plates passes over the mass transfer region, the governing equation for the mass transfer is as follows.

$$u\frac{\partial c}{\partial x} = D\left(\frac{\partial^2 c}{\partial x^2} + \frac{\partial^2 c}{\partial y^2}\right) \tag{1}$$

$$u = 6u_{ave}(1 - y/H)\,y/H \tag{2}$$

To solve the governing equation the dimensionless variables are chosen such as

$$X = x/6HPe$$

$$U = u/6u_{ave}$$

$$Y = y/H$$

$$\theta = (c - c_s)/(c_b - c_s) \tag{3}$$

where H is the distance between the plates, c_s is the concentration on the surface in the mass transfer region, c_b

* To whom all correspondence should be addressed.

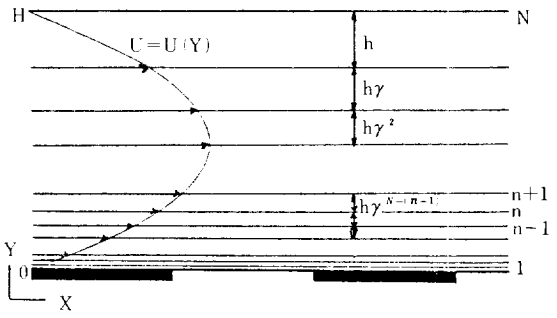

Fig. 1. The model of variational grid size.

is bulk concentration, u is the velocity in x-direction and u_{ave} is the mean velocity of u. Peclet number is defined as follows.

$$Pe=\frac{U_{ave}H}{D}=Re\cdot Sc \tag{4}$$

where D is the diffusion coefficient.
By substituting eq. (3) into eq. (1), we obtain

$$U\frac{\partial\theta}{\partial X}=\frac{\partial^2\theta}{\partial Y^2}+\frac{1}{36Pe^2}\cdot\frac{\partial^2\theta}{\partial X^2} \tag{5}$$

Leveque [8] has already obtained the general solution of the simplified eq. (5) with the assumption of linear velocity profile within the thin concentration boundary layer and neglecting axial diffusion. With the similar assumption of Leveque's the mass transfer equation for the tubular flow system with only mass transfer region was solved analytically by the other [9,10]. In order to obtain the more accurate numerical solution for the mass transfer system with the inert region, eq. (5) was solved numerically using the variational grid size technique. As shown in Fig. 1, when the ratio of two adjacent grid sizes is γ, eq. (5) can be transformed as follows.

$$U\frac{\theta_{i+1,n}-\theta_{i,n}}{\Delta x}=\frac{2\{\gamma\theta_{i+1,n+1}+\theta_{i+1,n-1}-(\gamma+1)\theta_{i+1,n}\}}{h^{2(N-n)}(1+1/\gamma)}+\frac{1}{36Pe^2}\frac{\theta_{i+1,n}-2\theta_{i,n}+\theta_{i-1,n}}{x^2}$$

$$U=\gamma\left(\frac{1-\gamma^{n-1}}{1-\gamma}\right)h\left(1-\gamma^{N-n}\frac{1-\gamma^{n-1}}{1-\gamma}h\right) \tag{6}$$

where i describes the X-directional grid element and n is the Y-directional grid element. In this study the number of grids was 801 and γ was 0.98.

When active and inert regions are arranged repeatedly, the boundary conditions for eq. (5) are given as follows.

$$\frac{\partial\theta}{\partial X}=0 \quad \text{at } X=0$$
$$\theta=1 \tag{7}$$

in the active region (Y = 0)

$$\theta=0 \tag{8}$$

in the inert region (Y = 0)

$$\frac{\partial\theta}{\partial Y}=0 \tag{9}$$

and at the upper plate (Y = 1)

$$\frac{\partial\theta}{\partial Y}=0 \tag{10}$$

Mass transfer rate in the active region is defined as follows.

$$Sh=\frac{\partial\theta}{\partial Y} \text{ at } Y=0 \tag{11}$$

With these boundary conditions eq. (6) is solved with the implicit marching step method.

RESULTS AND DISCUSSIONS

The concentration distributions on the active and inert regions help understand how the inert region affects the mass transfer process. Fig. 2 shows the concentration distributions for the case of RT = 1.0 where RT is the ratio of the inert area to the active area. When the concentration boundary was defined as the 99.9% of the bulk fluid concentration, it was shown that the concentration boundary layer also grew in the inert region as with the same trend as in the active region. Since the solute in the bulk diffused to the surface in the inert region regorously, the mass transfer rate in the next ac-

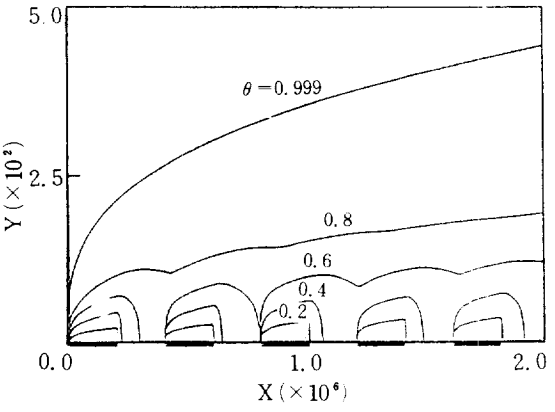

Fig. 2. Concentration layer distributions in active and inert regions (Pe = 165, Re = 100 and RT = 1.0).

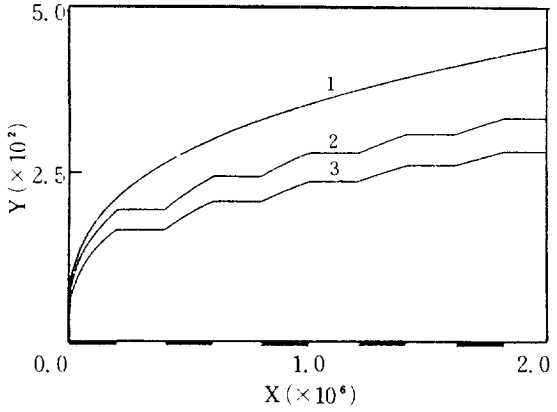

Fig. 3. Concentration boundary layer distributions.

1. numerical solution
2. with second-order concentration profile
3. with third-order concentration profile

tive region would be much affected. The concentration layer of $\theta = 0.8$ showed that the layer thickness decreased in the first inert region but slowly increased from the second region. These phenomena were more clearly at the lower concentration layers and then the concentration layer of $\theta = 0.2$ reached at the surface in the inert region. All the concentration layers, however, would reach at the surface if the length of the inert region were long enough.

According to Kim's mathematical model [7] the concentration boundary layer as shown in Fig. 3, did not grow in the inert region. His mathematical model showing the effect of the inert region on the mass transfer with the assumption of the third-order concentration profile was a good analytical approach but it could not consider the diffusion to the surface in the inert region because it is difficult to describe mathematically.

In Fig. 4 the local mass transfer rate distributions of the numerical solution were shown. Leveque solution and the analytical solution using the third-order concentration profile within the boundary layer were in good agreement with each other, but the analytical solution with second-order concentration profile had much higher mass transfer rate. The discrepancy in the case with second-order concentration profile is attributed to the fact that this profile does not include the non-slip condition of the concentration on the surface $(\frac{\partial^2\theta}{\partial Y^2})_{Y=0} = 0$ [6]. By means of the numerical analysis the effect of the inert region on the development of the concentration boundary layer was shown in Fig. 5. In spite of the increase of RT the thickness of the boundary layer decreased only slightly. This means that the solute is diffused to the surface in the inert region as much regorously as to that in the active region.

The mass transfer rates at Re = 100 and RT = 0.25 were shown in Fig. 6. The mass transfer rate obtained from the Leveque solution was denoted only for the active region along X-direction. The numerical solution showed that the mass transfer rate at the entrance of each active region increased suddenly due to the effect of the inert region. Both analytical solutions, however, did not show the sudden increase of the mass transfer rate because these two did not consider the diffusion to the surface in the inert region.

The local mean Sherwood numbers at each active region were shown in Fig. 7 for the same conditions of Fig. 6. This type of figure can be obtained from the direct

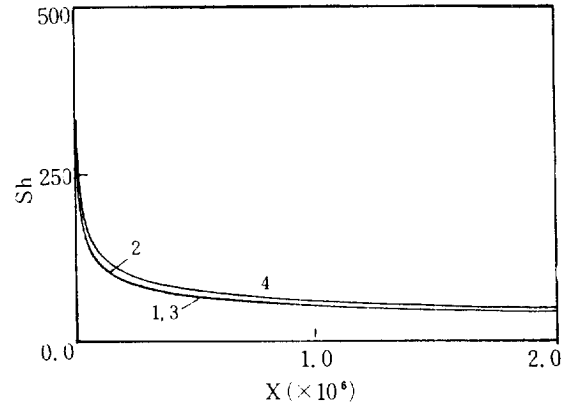

Fig. 4. Local Sherwood number distributions without inert region.

1. numerical solution
2. Leveque solution
3. with second-order concentration profile
4. with third-order concentration profile

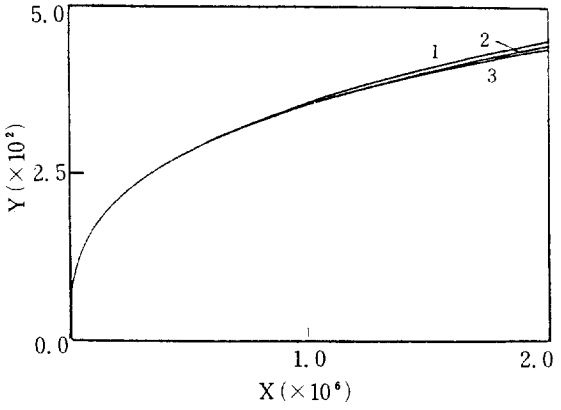

Fig. 5. Concentration boundary layer distributions by numerical solution.

1. RT = 0, 2. RT = 1.0, 3. RT = 2.0.

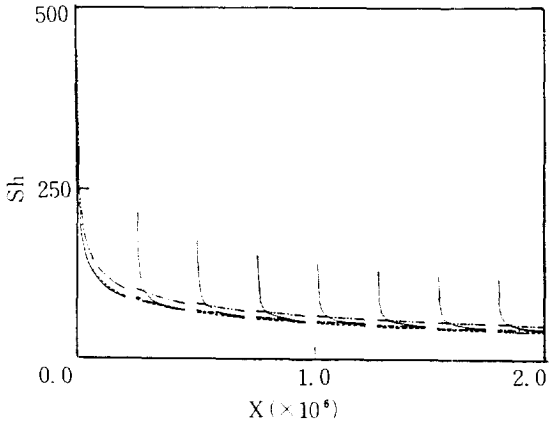

Fig. 6. Local Sherwood number distributions with inert region(Re = 100, RT = 0.25).

— : numerical solution
··· : Leveque solution
--- : with third-order concentration profile
—·—: with second-order concentration profile

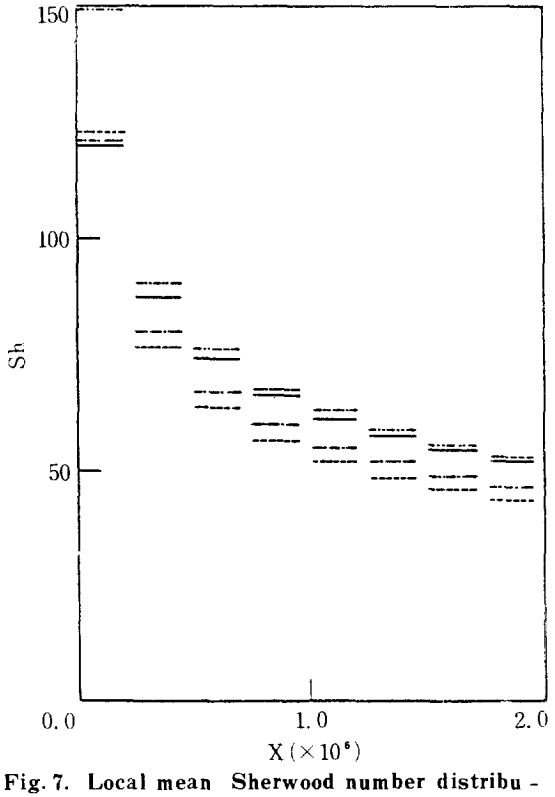

Fig. 7. Local mean Sherwood number distributions with inert region(Re = 100, RT = 0.25).

— : numerical solution
··· : Leveque solution
—·—: with third-order concentration profile
—··—: with second-order concentration profile

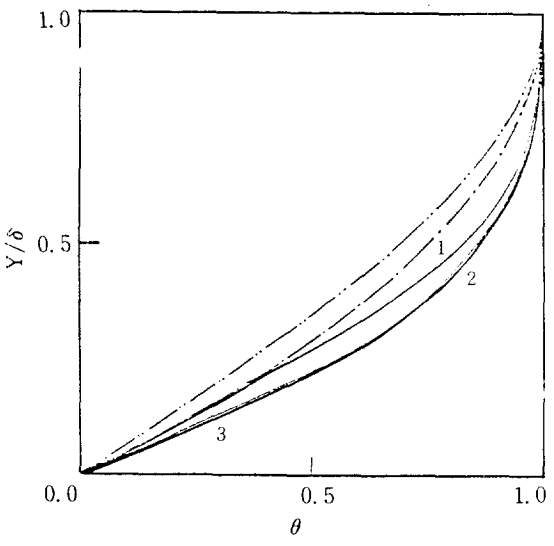

Fig. 8. Comparison of concentration profiles within concentration boundary layer.

—·—: third-order concentration profile
—··—: second-order concentration profile
—: numerical solution
1. at the end of the 1st active region
2. at the end of the 3rd active region
3. at the end of the 5th active region

measurements of mass transfer rate by using segmented electrodes. The local mean Sherwood numbers were compared with those obtained from Leveque solution, the numerical solution and the analytical solution using the third-order concentration profile, which were nearly the same in the first active region. But the local mean Sherwood number obtained from the analytical solution using the second-order concentration profile was much higher than any others in the all active regions.

The concentration profiles were shown in Fig. 8. The numerical solution showed that the concentration profile slightly changed at each active region.

In Fig. 9 and 10 the overall mean Sherwood number distributions as a function of Re and RT were shown respectively. When active and inert regions were arranged alternately to the distance of 2H, the overall Sherwood number Sh_m was obtained by $Sh_m = \dfrac{\int_0^{2H} Sh\, dx}{2H}$.

Here, each active length was 0.2H. Fig. 9 showed that the overall mean Sherwood number obtained from numerical analysis depends on Re with nearly same exponent of that obtained from the Leveque solution, but Fig. 10 showed that Sh_m depends on RT much more highly than the Leveque solution. The slight dependency of the Leveque solution on RT is due to the decrease of the total active area by the increase of RT.

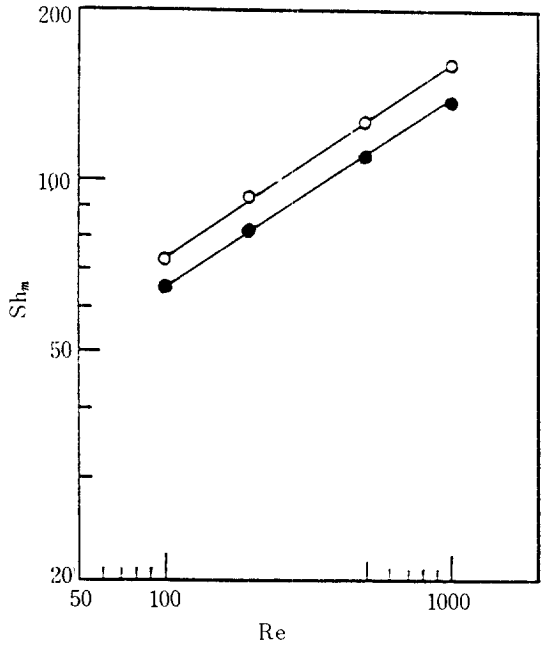

Fig. 9. Relation of mean Sherwood number with Reynolds number (RT = 0.25).

○ : numerical solution
● : Leveque solution

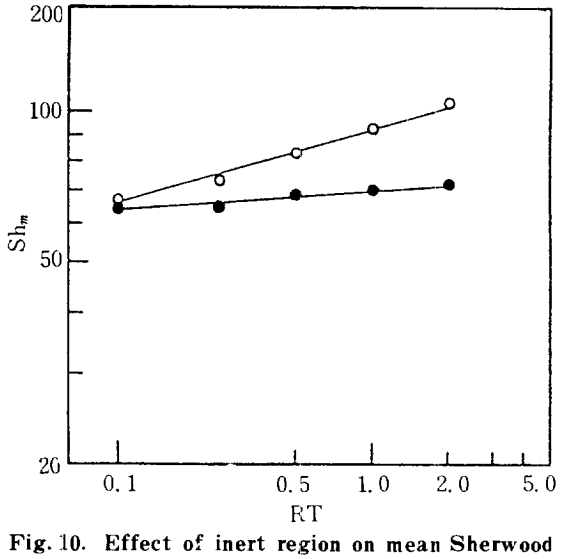

Fig. 10. Effect of inert region on mean Sherwood number (Re = 100).

○ : numerical solution
● : Leveque solution

As shown in Fig. 11 the overall mean Sherwood number that was obtained from the numerical analysis was correlated as follows.

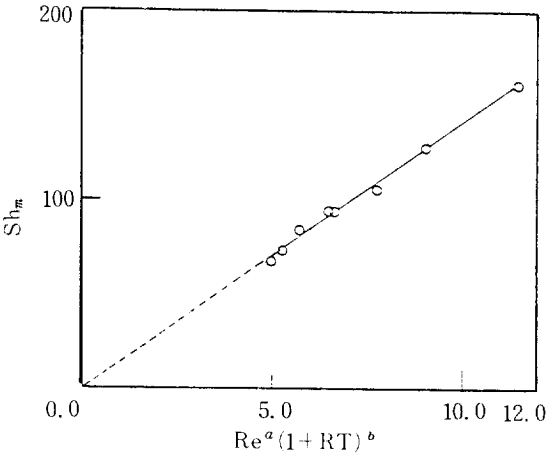

Fig. 11. Correlation for mean Sherwood number as a function of Reynolds number and area ratio (Sc = 1650) Re = 100, 200, 500 and 1000; RT = 0.1, 0.25, 0.5, 1.0 and 2.0; X = 0.339 and Y = 0.444.

$$Sh_m = 13.96\ Re^{0.339}(1+RT)^{0.444}$$

When Re was 100 and RT was 0.25, the overall mean Sherwood number was 12% greater than that of the Leveque solution and when Re was 100 and RT was 0.5, it was 23% greater than that of the Leveque solution.

CONCLUSION

The effect of the inert region on the mass transfer of the segmented electrodes was studied numerically using the variational grid size technique.

When the ratio of two adjacent grid sizes, γ was 0.98 and the number of grids was 801, the numerical analysis discribed well the concentration profile within the very thin concentration boundary layer in the short distance. The concentration boundary that had formed in the earlier active region also grew in the following inert region due to the diffusion. The diffusion in the inert region causes the greater mass transfer rate than expected. The mass transfer rate in the active region increased with the inert region.

The overall mean Sherwood number obtained from numerical analysis was correlated as follows.

$$Sh_m = 13.96\ Re^{0.339}(1+RT)^{0.444}$$

Since the effect of the inert region on the mass transfer depends strongly on the ratio of the inert area to the active area, it is recommended that electrodes be arranged within the range of RT = 0.25 for the smaller error than 12%.

NOMENCLATURE

c : Concentration
c_b : Concentration in Bulk
c_s : Concentration at Surface
D : Diffusivity
H : Characteristic Length (= Channel Height)
i : Grid Number in X-Direction
N : Total Number of Grids in Y-Direction
n : Grid Number in Y-Direction
Re : Reynolds Number
RT : Ratio of Inert Area to Active Area
Pe : Peclet Number
Sc : Schmidt Number
Sh : Local Sherwood Number
Sh_m : Overall Mean Sherwood Number
U : Dimensionless Velocity in X-Direction
U_{ave} : Mean Velocity of U
ΔX : Grid Size in X-Direction

Greek Letters

γ : Ratio of Two Adjacent Grid Sizes in Y-Direction
θ : Dimensionless Concentration
δ : Concentration Boundary Layer Thickness

REFERENCES

1. Lin, C.S., Denton, E.B., Gaskill, H.S. and Putnam, G.L.: *Ind. Egn. Chem.*, **43,** 2136 (1951).
2. Reiss, L.P. and Hanratty, T.J.: *AIChE J.*, **8,** 245 (1962).
3. Grassman P.P.: *Int. J. Heat Mass Trans.*, **22,** 795 (1979).
4. Chang, H.N., Park, J.K. and Kim, C.: *Int. J. Heat Mass Trans.*, **27,** 1922 (1984).
5. Sonin, A.A. and Probstein, R.F.: *Desalination*, **5,** 293 (1968).
6. Kim, I.H., Kang, I.S. and Chang, H.N.: *Desalination*, **33,** 139 (1980).
7. Kim, D.H.: Thesis, KAIST (1981).
8. Levich: "Physicochemical Hydrodynamics", Prentice-Hall, N.J. (1973).
9. Newman, J.S.: "The Fundamental Principle of Current Distribution and Mass Transportation in Electrochemical Cells", Electroanalytical Chemistry, N.Y. (1973).
10. Pickett, D.J.: "Electrochemical Reactor Design", Elsevier Scientific Publishing Company, N.Y. (1979).